Dynamics of the plasmasphere and the outer radiation belt from DMSP, IMAGE, and SAMPEX observations

W. R. Johnston[1], P. C. Anderson[1], J. Goldstein[2], and T. P. O'Brien[3]

[1]W. B. Hanson Center for Space Sciences, University of Texas at Dallas, Richardson, TX [2]Space Science and Engineering Division, Southwest Research Institute, San Antonio, TX [3]The Aerospace Corporation, Chantilly, VA

Abstract

During geomagnetic disturbances, the plasmapause and the outer radiation belt exhibit very dynamic behavior in terms of radial location and particle populations. These behaviors have been shown to be correlated as a result of wave-particle interactions contributing to outer radiation belt particle energization and loss. Efforts to model this relationship have been hampered by the limited temporal coverage of available plasmapause observations. We identify the signature of the plasmapause in the ionosphere, i.e. the light ion trough, from DMSP RPA observations, then map these locations along magnetic field lines to the equatorial plasmapause. This can offer over 10 years of plasmapause observations from multiple DMSP satellites. Our identifications compare well with those from IMAGE EUV observations. DMSP light ion measurements often show indications of plasmaspheric structure, e.g. notches and plumes, with such structure tending to account for differences between DMSP and IMAGE identifications. The DMSP-derived plasmapause is found to correlate with outer radiation belt dynamics, including locations of SAMPEX-observed precipitating particle microbursts.

Plasmasphere-radiation belt interactions

The Earth's plasmasphere is dynamically influenced by magnetospheric and ionospheric electric fields. The evolution of the plasmapause during active times can significantly affect the outer radiation belt:

- *Summers et al.* [1998] argue that enhanced electromagnetic ion cyclotron (EMIC) waves within the plasmasphere tend to scatter trapped electrons into the loss cone, depleting radiation belt particles inside the plasmapause. At the same time, outside the plasmapause whistler-mode waves tend to energize trapped electrons (**Fig. 1**).
- *Goldstein et al.* [2005] found that the outer radiation belt responded to radial movement of the plasma-pause during disturbed times with a time lag of several days.

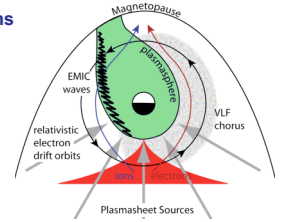

Fig. 1. Schematic of proposed mechanisms for outer radiation belt energization and loss associated with the plasmasphere. [From *Reeves,* 2007, after *Summers et al.,* 1998.]

Plasmapause-ionosphere interactions

Several ionospheric signatures of the plasmapause have been proposed, including:

- midlatitude electron density trough
- subauroral electron temperature enhancement (SETE)
- total electron content (TEC)
- light ion trough (LIT)
- precipitating electron boundary
- stable auroral red arcs (SARS)

In general, there is not a one-to-one correspondence between any of these and the plasmapause. *Taylor and Walsh* [1972] found LIT one of the more consistent signatures, whereas *Foster et al.* [1978] found the LIT generally a few degrees equatorward of the plasmapause as identified by whistler waves. *Grebowsky et al.* [1978] suggested supersonic upward H^+ flows result in LIT-plasmapause mismatch during refilling.

Precipitating particle microbursts

Microbursts are short duration (<1 sec) bursts of relativistic electrons observed by low altitude satellites. Using SAMPEX data *Nakamura et al.* [2000] showed microbursts were associated with the dawnside and with post-storm recovery of the depleted radiation belt. *Lorentzen et al.* [2001a] showed innermost microburst locations during storms tended to track modeled plasmapause location. Microbursts are believed to represent wave-particle scattering of energetic electrons into the loss cone, a side effect of whistler chorus energization of electrons outside the plasmapause. *Lorentzen et al.* [2001b] linked microbursts to VLF chorus observed by Polar, and *O'Brien et al.* [2003] linked microbursts to ULF activity at low L shells.

Satellites/instrumentation: DMSP, IMAGE, SAMPEX

DMSP: polar sun-synchronous orbits, alt. 840 km, period 100 min., generally 3-4 operational at any given time. During 2001 data is available from F12, F14, and F15 in pre-midnight to morning and F13 in dusk to dawn.

Instruments include:

- Retarding Potential Analyzer (RPA) providing ion density and composition
- Ion Drift Meter (IDM)
- Precipitating Electron and Ion Detectors (SSJ/4)

IMAGE: eccentric polar orbit (from 1400 km alt. to 8 R_E), operational 3/2000 to 12/2005. Instruments include:

- EUV imagers directly imaging 30.4 nm UV scattered by plasmaspheric He^+. Such imaging is feasible when IMAGE is near apogee (**Fig. 2**).

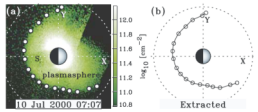

Fig. 2. Sample IMAGE EUV image of plasmasphere, showing extracted plasma-pause locations [from *Goldstein et al.,* 2004].

SAMPEX: low Earth orbit, operational 7/1992, alt. from 500 km to 620 km in 2001, includes four instruments for energetic particle measurements:

- Heavy Ion Large Area Proportional Counter Telescope (HILT)
- Low Energy Ion Composition Analyzer (LEICA)
- Mass Spectrometer Telescope (MAST)
- Proton/Electron Telescope (PET)

Method and validation

Our approach uses the DMSP-observed LIT as identification of the low-altitude plasmapause. The algorithm is illustrated in **Fig. 3**, with steps as follows (for free parameters, values used are in parenthesis):

1) DMSP H^+ density data for MLAT 20°-65° (N or S), 4-sec sampling;
2) smooth using Hanning window with fixed MLAT half width w (w=2°);
3) reject passes where dynamic range of resulting series is less than β (β=10); also manually reject some passes (e.g. too noisy, no LIT visible on day side);
4) identify all local minima in smoothed density;
5) identify subset of these minima with a steep equatorward rise in density (density at least 3x greater 5° equatorward);
6) proceed equatorward from each minima to location where density is higher than at minimum by factor f (f=1.3);
7) manually identify one such location as plasmapause (may manually identify multiple boundaries in structured cases).

Fig. 3

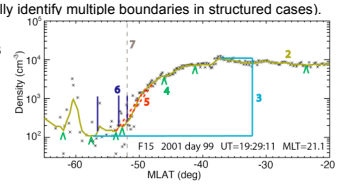

Applying this method to a 72-day period in 2001 (days 80-151), we obtained 2,392 plasmapause identifications, an average of 33 per day (range of 3 to 63 per day). This represents 15% of the DMSP passes in this period: 34% of passes were rejected automatically (step 3), and 50% were rejected manually before analysis. Most identifications were at dusk-midnight or predawn-dawn.

The plasmapause locations in the ionosphere are mapped along magnetic field lines to the equatorial plasmapause, using IGRF 2000 and Tsyganenko 2001 magnetic field models. Comparisons with SAMPEX may be done without mapping, since SAMPEX and DMSP are at similar altitudes.

Fig. 4 shows comparison of DMSP-identified plasmapause L values to IMAGE identifications using a previous algorithm version described by *Anderson et al.* [2008]. *Points ("error" bars)* show average (range) of IMAGE-extracted plasmapause locations within 15 min of time and 15 min of MLT of a DMSP identification. Comparisons form two clusters:

- *Filled circles* show main cluster (N=147, 79%) of good matches, with a mean L value difference of 0.45±0.43. *Red line* shows best fit for this cluster, *blue dashed line* represents identical L values.
- *Open circles* show second cluster of mismatches (N=40, 21%), with a mean L value difference of 1.78±0.45. Case-by-case examination of mismatches show that differences are often accounted for by highly structured plasmasphere conditions, including cases where DMSP is detecting plumes or notches.

Fig. 4

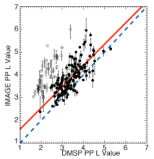

Fig. 5 illustrates one such mismatch case. Left plots show DMSP H^+ observations with extracted plasmapause *(red line)*, with three good matches and one mismatch (F15) within a 50 min. period. Right plot shows DMSP mapped orbit tracks *(red lines)* and DMSP plasmapause identifications *(red asterisks)* overlaid on an IMAGE observation projected onto the SM X-Y plane. The mismatch case maps to a plasmaspheric notch.

Fig. 5

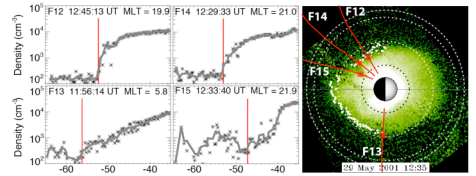

Plasmapause and microbursts

We have applied our method to days 80-151 of 2001, the same period for which *Goldstein et al.* [2005] examined dynamic behavior of the plasmapause and radiation belt:

Fig. 6 shows comparison of plasmapause locations to radiation belt flux for the 72-day study period:

- *Spectrogram* shows SAMPEX observations of 1.5-6 MeV electron flux for L value vs. day (daily average of 0.1-L bins).
- *Heavy white line* shows daily average plasmapause location from DMSP (not separated by MLT); *thin white lines* show one standard deviation range in daily plasmapause location.
- Upper plot shows Dst.

Each storm/disturbance produces rapid erosion of the plasmapause and depletion of the outer radiation belt (timescale ~1 day). Over following days the plasmapause moves outward with refilling and the outer radiation belt is repopulated. If the plasmapause overlaps the radiation belt, this may produce depletions of the radiation belt on timescales of days (e.g. after days 120 or 140).

Fig. 6

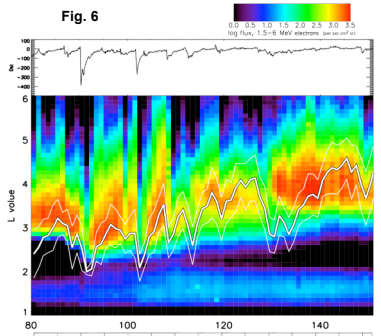

Fig. 7 compares DMSP-identified plasmapause locations *(black)* and daily average *(green)* and locations of SAMPEX observations of microbursts *(red)*, by bins of 0.25 L within which one or more microbursts were detected. Lack of microbursts during days 115-125 is from precession of SAMPEX into MLT sector where it is poorly positioned to detect them.

- Erosion-driven inward movement of plasmasphere is accompanied by prompt (timescale <1 day) inward movement of microburst locations, along with intensification.
- Microbursts are consistently located outside of the plasmapause, with isolated exceptions; this remains the case even on timescales less than a day.
- During plasmasphere refilling, innermost microbursts tend to be outward of plasmapause observations by ~0.5 L, suggesting a lower threshold in plasma density for microbursts than that for the DMSP-identified plasmapause.

Fig. 7

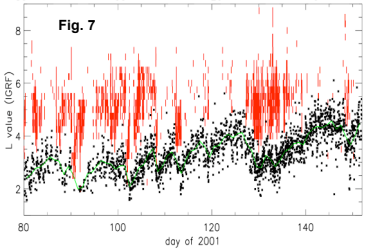

During stormtime erosion at a given L shell, the time delay between last plasmapause detection and first microburst detection provides some measure of the time scale for development of conditions producing microbursts. **Fig. 8** shows the cumulative fraction of observed cases (disturbance and L-shell) where this delay is less than or equal to a specified time. Observed microbursts increase at delays of ~3 hours.

Fig. 8

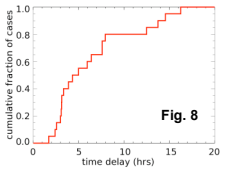

Conclusions and future work

- Our method of identifying the plasmapause using DMSP data compares well to IMAGE plasmapause observations; review of DMSP-IMAGE mismatch cases reveals that DMSP often observes plasmaspheric structure (e.g. notches, plumes) that account for mismatches.
- Comparison of locations for DMSP-identified plasmapause and SAMPEX-observed microbursts shows microbursts are consistently outside the plasmasphere, with correlations between locations of innermost microbursts and outermost plasmapause detections.
- During plasmasphere erosion, microburst locations move into emptied regions on short timescales; data suggests microbursts follow last plasmasphere detection by as little as ~3 hours.

This method is being applied to ~10 years of DMSP data, potentially providing ~100,000 plasmapause detections spanning a full solar cycle. Combined with SAMPEX data, the resulting database will be used to examine the relationship of the plasmasphere and radiation belt energization and loss.

Acknowledgements

We gratefully acknowledge our data sources: the SAMPEX Data Center, ACE Data Center, NASA IMAGE mission, the Kyoto Data Center for Dst data, and the Center for Space Sciences at the University of Texas at Dallas and USAF for DMSP data. This work is supported by NASA NESSF grant NNX07AU71H.

References

- Anderson, P. C., et al. (2008), submitted to *GRL*.
- Foster, J. C., et al. (1978), *JGR* 83:1175+.
- Goldstein, J., et al. (2004), *GRL* 31:L01801.
- Goldstein, J., et al. (2005), *GRL* 32:L15104.
- Grebowsky, J. M., et al. (1978), *Planet. Space Sci.*, 26:651+.
- Lorentzen, K. R., et al. (2001a), *GRL*, 28:2573+.
- Lorentzen, K. R., et al. (2001b), *JGR*, 106(A4):6017+.
- Nakamura, R., et al. (2000), *JGR*, 105:15875+.
- O'Brien, T. P., et al. (2003), *JGR*, 108(A8):1329+.
- Reeves (2007), RBSP Science Overview, THEMIS presentation.
- Summers, D., R. M. Thorne, F. Xiao (1998), *JGR*, 103(A9):20487+.
- Taylor, H. A., Jr., and W. J. Walsh (1972), *JGR* 77:6716+.